

Cite this: *Mater. Adv.*, 2026,
7, 3439

Confinement-driven equilibrium shifts in steam methane reforming: a monte carlo study in zeolites

Botagoz Zhakishева,^a Juan José Gutiérrez-Sevillano,^{id}*^{bc} Patrick J. Merkling^{bc}
and Sofia Calero^{id}*^{ab}

Steam methane reforming (SMR) remains the dominant industrial route for hydrogen production, yet its highly endothermic nature demands elevated temperatures, resulting in substantial energy input and CO₂ emissions. In this work, we investigate whether thermodynamic confinement within nanoporous materials can alter the confined-phase composition under SMR-relevant conditions and evaluate the potential equilibrium shift in coupled reaction-separation systems towards enhanced hydrogen production at lower temperatures. Using reaction ensemble Monte Carlo and grand Canonical Monte Carlo simulations, we validate our molecular models against experimental bulk-phase data, and then systematically compare confinement-induced composition changes in large- and small-pore zeolites. Our results reveal that large-pore zeolite FAU, in both hydrophilic (NaX) and hydrophobic (pure silica) forms, fails to outperform the bulk. In contrast, the small-pore zeolite ITQ-12 shows hydrogen enrichment in the confined phase. At 1 bar and 675 °C, ITQ-12 achieves hydrogen mole fractions comparable to those in the bulk at 825 °C, representing an apparent 150 °C reduction in temperature with potential for considerable energy savings. Zeolite RHO, despite similar pore size, shows no such improvement, highlighting the critical role of channel geometry and topological confinement. These findings demonstrate that properly selected zeolite topologies can thermodynamically steer SMR towards more sustainable conditions. The framework established here offers a predictive route to identify nanoporous materials capable of enabling low-temperature hydrogen production.

Received 5th December 2025,
Accepted 18th February 2026

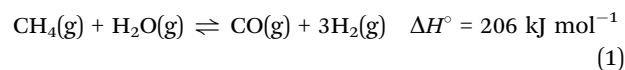
DOI: 10.1039/d5ma01416f

rsc.li/materials-advances

Hydrogen is a clean energy carrier that can store and deliver energy flexibly. Its main uses are in refining, the chemical sector (ammonia and methanol production) and steel manufacturing (to produce iron *via* the direct reduced iron route using fossil-based synthesis gas). Hydrogen has great potential in emerging application markets such as long-range transportation (ship or plane) and energy storage. There are many ways to produce hydrogen, including production from fossil fuels and renewable resources. One of the most important and commonly used industrial processes to produce hydrogen and synthesis gas is steam methane reforming (SMR) which is used to produce mostly grey hydrogen and a very small proportion of blue hydrogen.¹ The process accounts for about two thirds of the world's total mass production of hydrogen.¹

For the U.S., this figure lies currently at 95%.² This mature technology is currently an economical way of producing hydrogen and is playing a role in the early stages of the hydrogen economy.²

Following Le Chatelier's principle, the reaction is favored under conditions of high temperature and low pressure. In conventional reformers methane reacts with water vapor under harsh operating conditions (1073–1273 K and 14–20 bar) in the presence of a catalyst, typically Ni, producing hydrogen and carbon monoxide. The steam methane reforming reaction to produce syngas is strongly endothermic:



It has been reported in previous studies that chemical reactions could be conducted advantageously in a porous material.^{3,4} In it, the confinement effect may increase the yield of the reaction products due to an increased density in the pores. Importantly, the degree to which confinement affects equilibrium is strongly dependent on the geometry and

^a Department of Applied Physics, Eindhoven University of Technology, 5600 MB Eindhoven, Netherlands. E-mail: scalero@tue.nl^b Department of Physical, Chemical and Natural Systems, Universidad Pablo de Olavide, Seville, Spain. E-mail: jjgutierrez@upo.es^c Center for Nanoscience and Sustainable Technologies (CNATS), Universidad Pablo de Olavide, Seville, Spain

connectivity of the porous framework. While pore volume and size are often cited and some works study the effect of cations present in the pores,⁵ the topological constraints, such as the dimensionality and curvature of the channel network, can introduce entropic penalties or enhancements that shift the equilibrium in non-trivial ways. Understanding these topology-driven effects is essential for rational material selection. Thus, X. Peng *et al.* in their study of steam methane reforming reaction equilibria in activated carbons have concluded that the yield of hydrogen in the pores could not be improved in these systems even if they varied the separation between layers.⁶ Experimental validation of reaction equilibria under confinement is extremely challenging due to the high temperatures, complex diffusion processes, and structural instability of some materials under working conditions. Therefore, molecular simulations offer a critical pathway for systematically exploring a large set of candidate materials and for revealing trends that can guide experimental efforts. In particular, we focus on thermodynamic descriptors that can be efficiently computed and scaled to large databases of hypothetical materials. In this work, we show that specific zeolite topologies with narrow, one-dimensional channels can significantly alter the confined-phase composition of the SMR species, leading to preferential hydrogen retention in the pores at lower temperatures. By combining atomistic simulations with topological descriptors, we identify structural motifs that favor enhanced performance, offering a predictive framework for shape-selective design in confined reaction environments.

1 Methodology

To investigate the influence of confinement on the equilibrium of the steam methane reforming (SMR) reaction, we performed molecular simulations that combine atomistic precision with thermodynamic rigor, enabling us to quantify confinement-induced changes in composition under realistic process conditions. The steam methane reforming reaction has been simulated in the bulk using a combination of the Monte Carlo method in reaction ensemble with the continuous fractional component Monte Carlo technique⁷ using the code RASPA.⁸ This approach was selected due to its robustness for simulating chemical equilibrium in multicomponent gas mixtures within rigid porous materials. RASPA's reaction ensemble Monte Carlo (RxMC) method, coupled with continuous fractional component Monte Carlo (CFCMC), is particularly suited to simulate endothermic reactions such as SMR in confined environments, where standard kinetic models are insufficient. The Monte Carlo method in the reaction ensemble is an atomistic approach that was developed to establish the equilibrium of a chemical reaction. It makes use of a Monte Carlo 'reaction' move that samples the reaction forward and backward respecting reaction stoichiometry. The 'reaction' MC move randomly selects reagent or product molecules in stoichiometric proportions to remove from the reaction mixture and inserts product or reagent molecules, respectively. It thus

comes down to combinations of particle creation and destruction moves which are chosen with equal probability to ensure microscopic reversibility is kept. The method requires the input of partition functions of each molecule in the gas phase and, applying the constraints of the simulation, establishes the equilibrium distribution in the confined environment.⁹ The Monte Carlo simulations in the reaction ensemble were integrated with the continuous fractional component Monte Carlo (CFCMC) method to improve the efficiency of the insertion/deletion Monte Carlo trial moves. The method is purely thermodynamic and thus does not take into account the activation energy barrier or the mechanism, but directly minimizes the Gibbs free energy. The ideal gas partition function can be calculated forming the product displayed in eqn (2):

$$\frac{q_i(T)}{A_i^3} = \left(\frac{2\pi M_i k_B T}{h^2}\right)^{3/2} \frac{\pi^{1/2}}{\sigma_i} \left(\frac{T^3}{\theta_{\text{rot}A,i} \theta_{\text{rot}B,i} \theta_{\text{rot}C,i}}\right) \times \prod_{j=1}^{3N-6} \frac{1}{1 - \exp\left(-\frac{\theta_{\text{vib},j,i}}{T}\right)} g_{e1,i} \exp\left(-\frac{D_{0,i}}{k_B T}\right) \quad (2)$$

where i refers to the molecule focused on, A_i is its de Broglie wavelength, M_i its mass, k_B the Boltzmann constant, h the Planck constant, and T is the temperature. The external symmetry number σ_i is 12 for CH₄, 1 for CO and 2 for H₂O and H₂, $\theta_{\text{rot}A,i}$, $\theta_{\text{rot}B,i}$, $\theta_{\text{rot}C,i}$ are the characteristic rotational temperatures of the three principal moments of inertia, and $\theta_{\text{vib},j,i}$ is the j th mode vibrational temperature of molecule i . $g_{e1,i}$ is the degeneracy of the electronic ground state (equals 1 for all the molecules in this study), and D_0 is the atomization energy at 0 K. The data have been taken from reference.¹⁰

In a previous study on improving ammonia production, Matito-Martos, *et al.*⁴ proposed that grand canonical Monte Carlo (GCMC) simulations using the equilibrium composition obtained *via* reactive Monte Carlo (RMC) could be used to study confinement effects instead of RMC simulations and providing results that do not vary between methods. In the current study, we adopt the same methodology. To simulate confinement effect on the SMR reaction we performed Monte Carlo (MC) simulation in the grand-canonical ensemble (GCMC). The initial equilibrium composition of the reacting mixture was defined by the mole fractions of the reaction components obtained by RxMC method in the bulk. In the GCMC ensemble the chemical potential, volume, and temperature are fixed (μ VT), whereas the number of adsorbed molecules fluctuates. The fugacity is related to chemical potential and pressure is related to fugacity by fugacity coefficient using Peng–Robinson EOS. To change the number of molecules in the system the 'swap' MC move that randomly performs insertion or deletion of molecules with an equal probability of 50% was used. The other thermalization moves such as translation, rotation, and reinsertion were used. The simulations of confinement and adsorption of mixture also included the 'identity change' Monte Carlo moves.

Our simulations have been set to run for 50 000 initialization, 50 000 equilibration and 100 000 production cycles. Every



cycle in the RASPA code performs as many moves as there are particles in the system, with a minimum of 20 moves. The model assumes that molecules and zeolites are rigid. When more than one form was available such as in the case of zeolite ITQ-12, the high-temperature form was used.¹¹ This choice reflects the typical operating range of industrial reformers and ensures structural stability during the simulation, avoiding phase transitions that would introduce artifacts in the computed thermodynamics. Non-bonding van der Waals interactions are modeled using Lennard-Jones potentials, truncated at truncated at 12 Å and shifted to zero at the cutoff. Electrostatics are accounted for using the Ewald summation technique with relative precision of 1×10^{-6} . Periodic boundary conditions were applied in all three directions of space. The unit cell side lengths were chosen to be at least twice the cutoff distance size (12 Å).

We have used the model of Garcia-Sanchez *et al.*¹² to assign point charges to zeolite atoms. According to this model, the point charges that define the oxygen atoms connected solely to silicon O_{Si} and the oxygen atoms connected to aluminum O_{Al} differ. The distribution of aluminum atoms in the zeolite was done obeying Lowenstein's rule that forbids Al–O–Al bonds. We placed Na^+ extra-framework cations to balance the net negative charge in aluminum-substituted zeolite FAU. The cations were placed randomly and were allowed to move by random Monte Carlo translation trial moves. The model for water,¹³ has been taken from the literature, and used in conjunction with the models developed by our group for methane,¹⁴ carbon monoxide,¹⁵ and hydrogen.¹⁶ These models have been validated independently in previous adsorption and equilibrium studies, both at low and high temperatures, ensuring their transferability to the current system. All simulations in this study adhere to a consistent force field and charge scheme, facilitating comparison across zeolite topologies. Thus, methane is modeled as a united atom Lennard-Jones potential without charge. The model has been validated by our group to reproduce experimental adsorption isotherms on different types of zeolites.¹⁴ For water, the five-site Tip5pEw potential was employed, which is a Tip5p potential reoptimized for use with the Ewald summation method. The model was reported to be suitable for adsorption studies and was validated in our previous study of the heats of adsorption in X and Y zeolites.¹⁷ Carbon monoxide is modeled with Lennard-Jones parameters and point charges assigned to all their atoms. The model also includes a charged dummy atom without mass to reproduce the experimental dipole moment of the molecule (0.112 D). It has been validated to reproduce experimental adsorption in both pure silica and alumino-substituted zeolites at cryogenic and high temperatures.¹⁵ The model of H_2 is uncharged and described by a single Feynman–Hibbs Lennard-Jones interaction center and the interaction parameters with zeolites were taken from the work of Deeg *et al.*¹⁶ This model was previously tested and used in a couple of studies of hydrogen in zeolites.^{18,19} All point charges and Lennard-Jones parameters used in this work are summarized in Table S1 of the SI, with the exception of the Lennard-Jones parameters for the guest–guest

interactions, which were obtained applying Lorentz–Berthelot mixing rules. The conditions used in this work correspond to a molar steam to methane (S/C) ratio of one in the feed.

2 Results and discussion

To evaluate the potential of confinement-driven enhancements, we first validate our molecular models in the bulk phase and then systematically compare confined-phase compositions across zeolite topologies with varying pore sizes and chemistries. This two-step approach allows us to isolate topological effects and identify structures that enable hydrogen production at lower temperatures. In order to test the suitability of the models, we have computed the densities of each of the reactant and product molecules in the bulk at several working conditions (698–1198 K and 20 bar). As shown in Fig. 1, the simulated densities of H_2 , CH_4 and CO are in excellent agreement over the whole range of temperatures considered with the experimentally reported densities taken from the NIST database²⁰ (H_2) and with those from thermodynamic calculations using the Peng–Robinson equation of state²¹ (CH_4 and CO). In the case of water, there is a slight and systematic underestimation of the density in comparison with the data from the NIST database. However, taking into account the complex nature of the water molecule, extreme conditions of the operation and the wide range of temperatures studied, the match is satisfactory. These results provide strong support for the accuracy of the molecular models under the extreme temperature and pressure conditions relevant to industrial SMR processes.

In a second step, we validate the force field and models by performing a Monte Carlo simulation of the SMR reaction in the bulk in the reaction ensemble. To this purpose, partition functions are calculated analytically.¹⁰ The results are shown in Table 1. It can be seen from the table that the decrease in the partition functions of the products as temperature increases is less than the decrease of the reactants, which explains the increase in the equilibrium constant. This trend arises because the partition function of methane, which dominates the reactant side, decreases more steeply with temperature than those of the products. This imbalance shifts the equilibrium towards product formation as temperature increases, consistent with Le Chatelier's principle.

From the mole fractions obtained *via* RMC simulations, we calculate the equilibrium bulk constants K_p of the reaction and the CH_4 conversions and compare them with the experimentally reported values.

As Fig. 2 shows, the equilibrium constants of the SMR reaction in the bulk calculated from the simulations are in very good agreement with those from the literature.²² The conversions of methane in the bulk, as shown in Fig. 3, calculated at pressures of 1 and 20 bar and stoichiometric conditions are in excellent agreement with the experimental data.²² This shows that the bulk properties are well reproduced by the simulations. The strong agreement between simulation and experimental equilibrium constants and conversions confirms that our



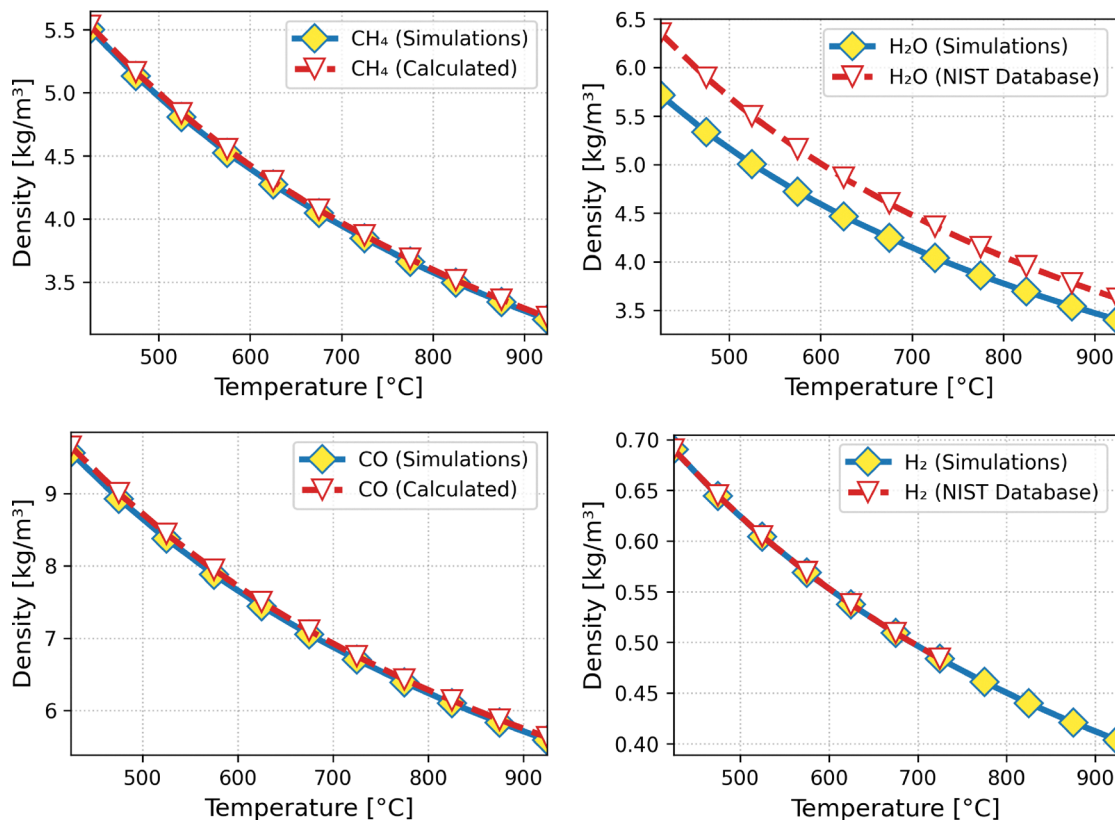


Fig. 1 Densities at 20 bar of the pure substances methane (top left), water (top right) carbon monoxide (bottom left) and hydrogen (bottom right).

Table 1 Partition functions, more specifically $\log(q_i(T)/\Lambda_i^3)$, in which q is the partition function and Λ is the de Broglie wavelength of the molecules involved at a few representative temperatures

$T/^\circ\text{C}$	CH_4	H_2O	CO	H_2
625	105.582	63.445	72.731	32.109
675	100.681	60.730	69.534	30.866
725	96.280	58.293	66.661	29.752
775	92.308	56.093	64.067	28.747
825	88.707	54.099	61.713	27.838

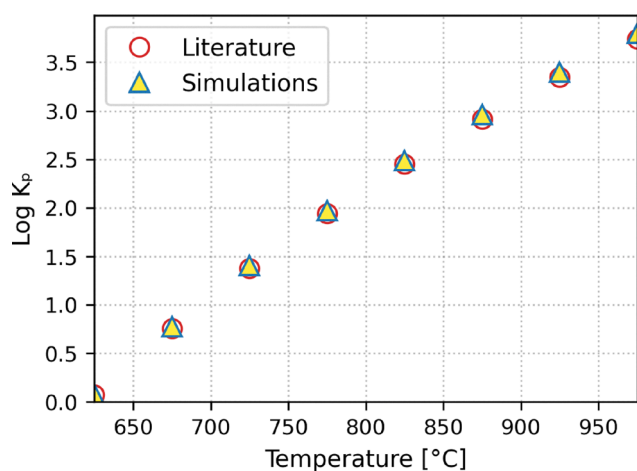


Fig. 2 Equilibrium constant of the SMR reaction as a function of temperature.

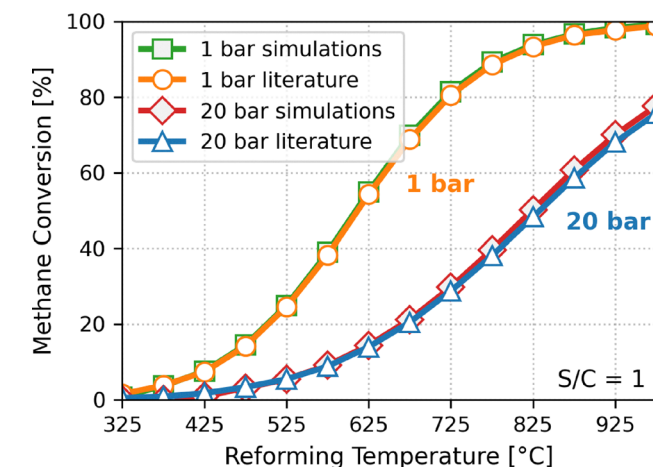


Fig. 3 CH_4 conversion percentage as a function of temperature.

simulation protocol captures the reaction Gibbs free energy governing the SMR equilibrium with high fidelity.

Once the force field and the models have been validated, we analyze the confinement effects on the SMR system. For this purpose, a zeolite widely used in industrial applications, faujasite (IZA²³ three-letter code FAU), has been selected. We use it in its all-silica form (Si/Al ratio ∞), and in its NaX form (Si/Al = 1). The setup assumes that the zeolite is in contact with a 1:1 CH_4 : H_2O feed to replenish those of the reagents that have been reacted away. Bulk-phase reactive equilibrium compositions for



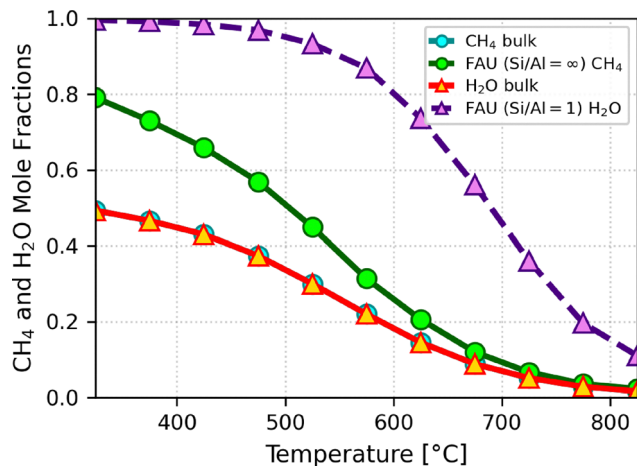


Fig. 4 CH_4 and/or H_2O mole fractions for the SMR reaction in faujasite and in the bulk at 1 bar.

this feed are obtained *via* RMC and used to define initial composition for the subsequent GCMC simulations in zeolites. To characterize confinement effects, Fig. 4 shows the mole

fraction of whichever of the reactants is more abundant in the zeolite, methane or water, at a pressure of one bar.

Faujasite NaX is hydrophilic, and consequently the mole fraction of water inside the zeolite is overwhelmingly higher than the one of methane. This might contribute to explain the poor results for this zeolite. The all-silica faujasite on the contrary is hydrophobic, and therefore the mole fraction of methane inside the zeolite is notably higher than the one of water. In this case as well, the use of a zeolite does not present an advantage over the bulk. These findings indicate that the large pore diameter of faujasite, combined with its lack of shape confinement, does not provide the steric or entropic constraints needed for preferential hydrogen retention. Additionally, the hydrophilicity of NaX further suppresses methane uptake, reducing reaction effectiveness.

All in all, it is clear from the results that the confinement in faujasite does not improve the hydrogen retention from the reaction equilibrium mixture.

However, faujasite with its pore diameter larger than 11 Å and its accessible diameter of 7.35 Å is a large pore zeolite. Hints of an improvement in methane conversion and hydrogen production below a threshold pore width of approximately 8.5 Å

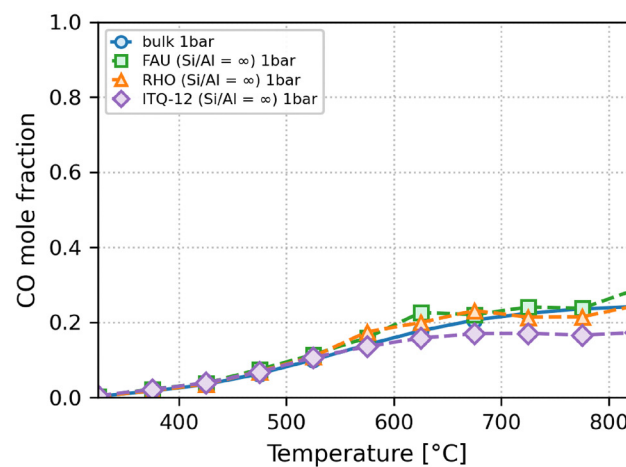
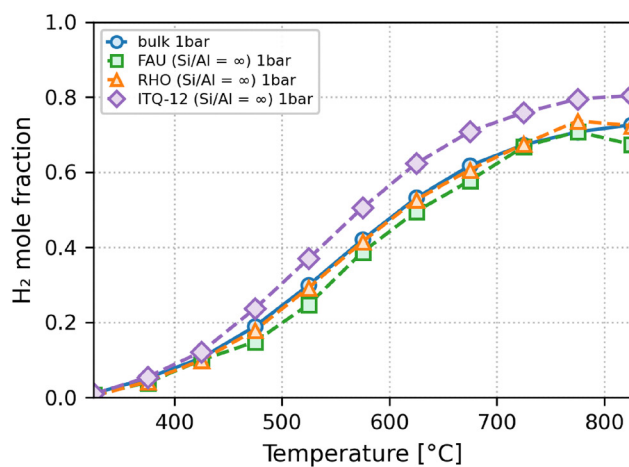
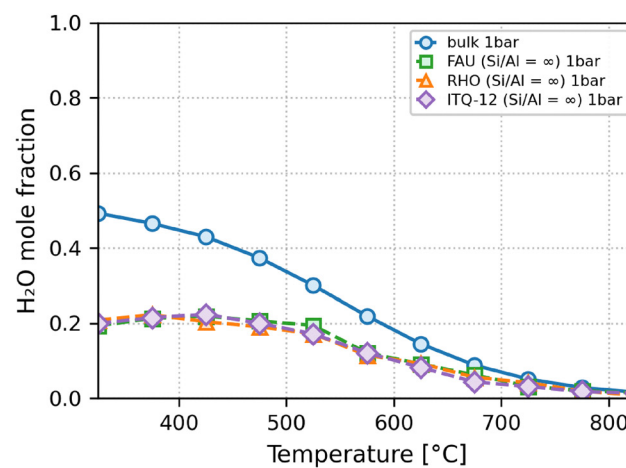
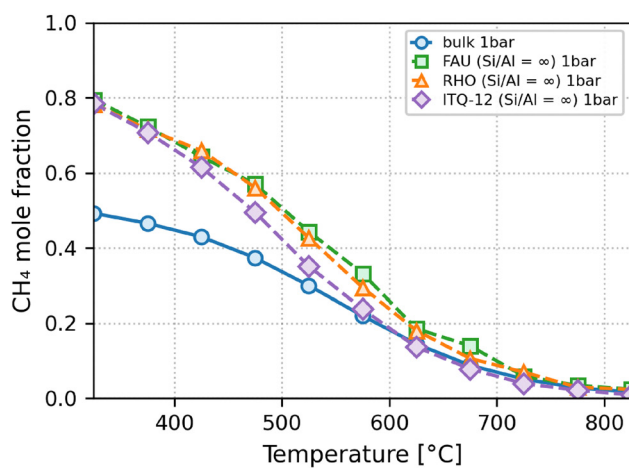


Fig. 5 Mole fractions of CH_4 (top left), H_2O (top right), H_2 (bottom left) and CO (bottom right) at equilibrium within zeolites FAU, RHO, ITQ-12 and in the bulk at 1 bar.



can be found in the work of Peng *et al.*,⁶ even though these authors did not get to narrow enough pores to observe an improvement over the bulk performance. Also, their system is made of flat sheets of graphite, which does not provide such an effective stabilization through adsorption of the reactants and products of the reaction than a channel-like or spherical pore would. To test whether enhanced confinement within narrower pores can promote hydrogen production, we next explore the behavior of two small-pore zeolites, RHO and ITQ-12 (which has an ITW topology), which exhibit sub-angstrom differences in accessible diameter and distinct channel geometries. We selected these two zeolites with small pore sizes in their all-silica form. Zeolite RHO consists of a combination of double 8-membered rings (d8r) and lta cages^{24,25} and has an accessible diameter of 4.06 Å.²³ The ITQ-12 structure consists of interconnected cavities and channels involving 8-membered rings. It forms two types of channels: the first, along the (100) direction is interrupted by slit-shaped 8-membered ring windows of dimensions 2.4×5.3 Å.²⁶ The second extends along the (001) direction, is rounder (3.8×4.1 Å) and connects bigger cavities. We expect this to enhance the selective adsorption of hydrogen and therefore increase its retention under confinement; in

reaction-separation systems this could shift the effective equilibrium towards the production of molecular hydrogen. Zeolite ITQ-12 has been shown in experimental studies to be able to separate carbon dioxide from methane²⁷ or propane from propylene.²⁸ Thus, the confinement effects were simulated inside the small-pore zeolites at several temperatures at a pressure of one bar.

In Fig. 5, the mole fractions of the reactants and products of the SMR reaction are displayed for the bulk and for the confined phase within zeolites FAU, RHO and ITQ-12 of pure silica composition. At temperatures well below 400 °C, the system remains strongly dominated by reactants even in the small-pore zeolites, in which the confined-phase consists of roughly 80% methane and 20% water with negligible amounts of products. In all cases, temperature is an enabler of the reaction. Thus, at temperatures above 550 °C, for zeolite ITQ-12 and above roughly 600 °C for the other zeolites examined, hydrogen mole fractions rise above 50%. Methane mole fractions at these temperatures reach similarly low levels to those in the bulk. On the contrary, water mole fractions are lower than the methane ones at these temperatures, and lower than they are in the bulk. Interestingly, unlike hydrogen, carbon

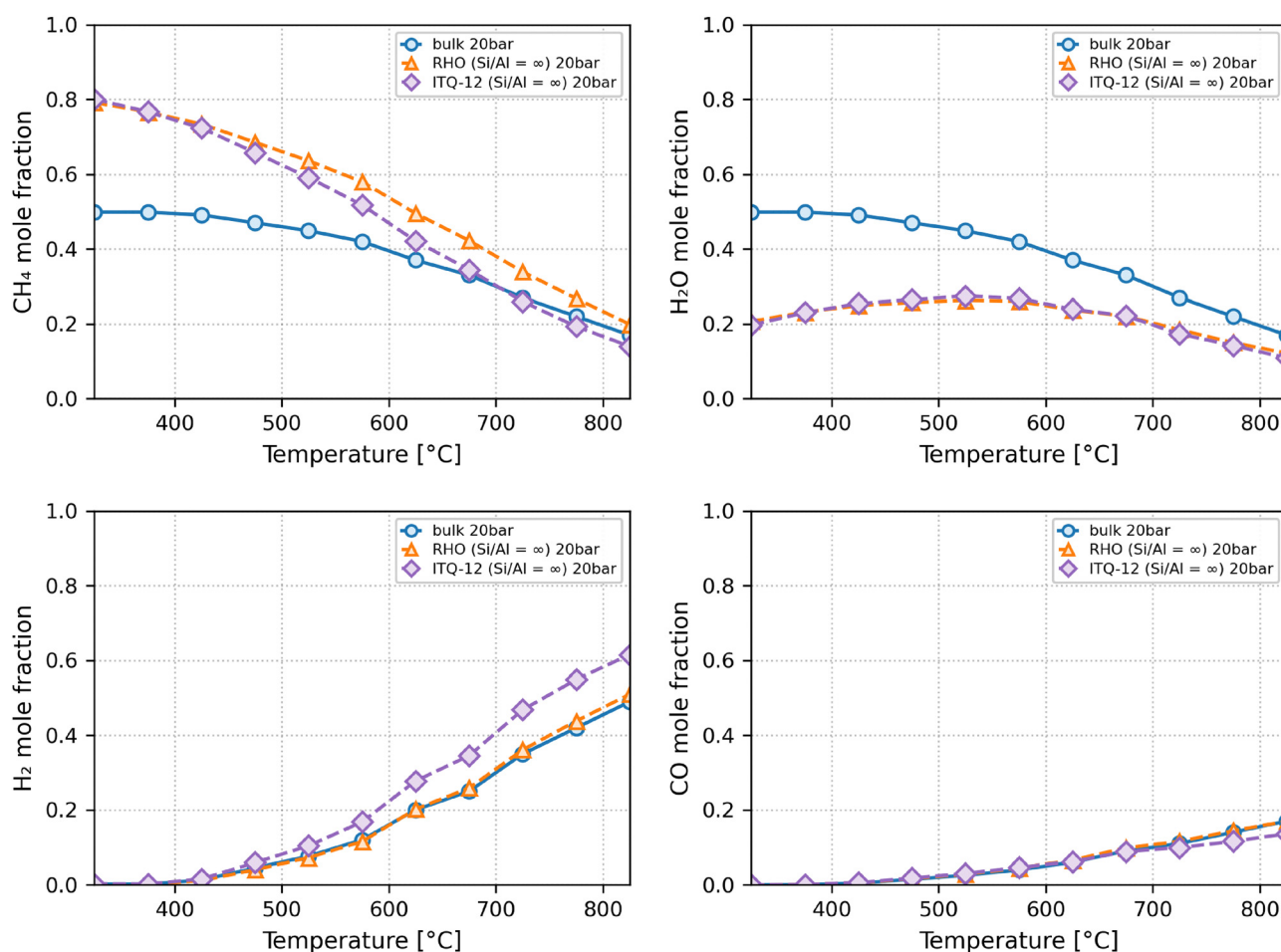


Fig. 6 Mole fractions of CH₄ (top left), H₂O (top right), H₂ (bottom left) and CO (bottom right) at equilibrium within zeolites RHO, ITQ-12 and in the bulk at 20 bar.



monoxide levels of the best-performing zeolite ITQ-12 are in fact lower than the ones of the bulk or the other zeolites, indicating that these molecules are expelled to the reservoir. Further, the figure shows that the hydrogen mole fractions obtained in the confined-phase increase marginally in zeolite RHO over zeolite FAU, and are similar to the levels in the bulk. In zeolite ITQ-12 however, a noticeable increase is achieved both compared to the other zeolites and to the bulk. Notably, the hydrogen mole fractions under the confinement of ITQ-12 zeolite at 675 °C is comparable to that in the bulk phase 825 °C. This suggests that, in a coupled reaction-separation configuration, ITQ-12 could help achieve similar hydrogen levels at substantially reduced operating temperatures of 150 °C lower than the bulk phase, representing a significant potential for process intensification and energy savings. Many zeolite structures remain thermally stable at temperatures as high as 800 °C and the Si/Al ratio correlates positively with higher thermal stability.²⁹ To the best of our knowledge the ITQ-12 case or indeed any member of the ITW family have not been studied in this regard. However, the mechanical stability of ITQ-12 is good,³⁰ which can be taken as a proxy for thermal stability.

At a higher pressure of 20 bar, more typical of the operating conditions in reactors, according to thermodynamics the reaction in the bulk is shifted to the reactant side, but how big is the effect in confinement? The comparison of Fig. 5 and 6 shows that in ITQ-12, in order to achieve a 0.5 mole fraction of hydrogen or a 0.1 mole fraction of CO requires a temperature increase of roughly 150 °C, from 575 to 725 °C or from 525 to 675 °C, respectively. At 20 bar, the advantage of ITQ-12 is partially retained: achieving a hydrogen mole fraction of 0.5 requires 725 °C, still 100 °C lower than the 825 °C needed in the bulk. While the pressure reduces the impact of confinement, ITQ-12 still enables measurable thermodynamic gains. In other words, whereas at 1 bar the use of zeolite ITQ-12 obtained similar mole fractions of hydrogen running the reaction 150 °C lower than in the bulk (825 → 675 °C), at 20 bar the temperature can only be lowered by 100 °C (825 → 725 °C). The analysis of these results can be further refined by representing the relative improvements at a pressure of 20 bar achieved by ITQ-12 over the bulk (Fig. S1 of the SI), in which hydrogen retention improvements are in the 34–40% range from 525 to 725 °C. Analyzing this figure together with Fig. 6, at a temperature of 675 °C, which we consider the optimum temperature at 1 bar, achieves very good improvement over the bulk (38%), the hydrogen mole fraction lies, however, below 0.4. At 725 °C, the increase over the bulk lies at 34%. Although higher temperatures would be desirable and still provide some benefits over the bulk, questions about long-term stability emerge.

From the comparison of the results at 20 bar and at 1 bar, the lower pressure is much preferred. The relative improvement achieved by ITQ-12 over the bulk at a pressure of 1 bar is shown in Fig. 7. The highest improvements are achieved at temperatures around 500 °C, at which a 24–25% improvement is observed, but this still corresponds to relatively modest hydrogen mole fractions of between 0.2 and 0.4. A separation may be envisaged, but would require a good purification scheme such

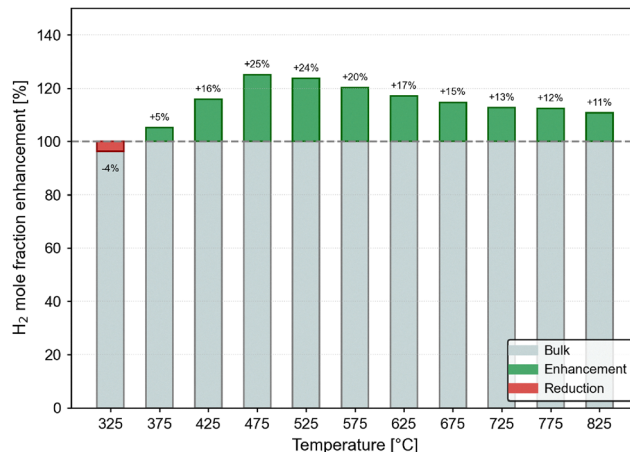


Fig. 7 Percentage improvement in the confined-phase H₂ mole fraction in ITQ-12 over the bulk at 1 bar.

as the one proposed recently.³¹ At 675 °C, the recommended operating temperature at 1 bar, potential enhancement of confined-phase hydrogen mole fraction over the bulk is still 15%. As temperatures increase and the systems tend towards saturation, the enhancement gets less significant.

3 Conclusions

We have investigated confinement effects on the steam methane reforming (SMR) reaction by combining reaction ensemble Monte Carlo simulations with grand canonical Monte Carlo simulations. Compared to the bulk phase, zeolite FAU—both in its hydrophobic and hydrophilic forms—shows reduced hydrogen mole fractions in the pores, highlighting that large-pore frameworks offer no advantage for this application. In contrast, among the small-pore zeolites examined, pure-silica ITQ-12 exhibits significantly enhanced performance. While zeolite RHO shows confined-phase compositions similar to the bulk and is thus not a promising candidate for process intensification, ITQ-12 exhibits pronounced hydrogen enrichment under confinement, indicating potential for reduction in reaction temperature. At 1 bar, hydrogen mole fractions in ITQ-12 at 675 °C match those obtained in the bulk at 825 °C, suggesting the potential for considerable energy savings. These findings demonstrate that channel geometry and pore size can be leveraged for selective hydrogen retention under SMR equilibrium conditions, which would shift the thermodynamic equilibrium of the SMR reaction.

Author contributions

B. Zhakisheva: writing – review & editing, writing – original draft, visualization, investigation, methodology, validation. J. J. Gutierrez-Sevillano: writing – review & editing, methodology, supervision, conceptualization. P. J. Merklings: writing – review & editing, methodology, conceptualization, supervision. S. Calero: writing – review & editing, methodology, supervision, resources, project administration, funding acquisition.



Conflicts of interest

There are no conflicts to declare.

Data availability

Data for this article, are available at Zenodo at <https://doi.org/10.5281/zenodo.17848102>.

Acknowledgements

This study was funded by the Spanish Ministerio de Ciencia e Innovacion (IJC2018-038162-I). We thank C3UPO for the HPC support.

Notes and references

- Global Hydrogen Review 2024, 2024, <https://www.iea.org/reports/global-hydrogen-review-2024>, Licence: CC BY 4.0.
- <https://www.energy.gov/eere/fuelcells/hydrogen-production-processes>, Retrieved 30/04/2025.
- C. H. Turner, J. K. Johnson and K. E. Gubbins, *J. Chem. Phys.*, 2001, **114**, 1851–1859.
- I. Matito-Martos, J. García-Reyes, A. Martín-Calvo, D. Dubbeldam and S. Calero, *J. Phys. Chem. C*, 2019, **123**, 18475–18481.
- B. Zhakishcheva, J. J. Gutiérrez-Sevillano and S. Calero, *Microporous Mesoporous Mater.*, 2025, **385**, 113480.
- X. Peng and Q. Jin, *Int. J. Hydrogen Energy*, 2022, **47**, 7569–7585.
- A. Poursaeidesfahani, R. Hens, A. Rahbari, M. Ramdin, D. Dubbeldam and T. J. H. Vlugt, *J. Chem. Theory Comput.*, 2017, **13**, 4452–4466.
- D. Dubbeldam, S. Calero, D. E. Ellis and R. Q. Snurr, *Mol. Simul.*, 2016, **42**, 81–101.
- C. H. Turner, J. K. Brennan, M. Lisal, W. R. Smith, J. Karl Johnson and K. E. Gubbins, *Mol. Simul.*, 2008, **34**, 119–146.
- D. A. McQuarrie, *Statistical Mechanics*, Harper and Row, New York, 1976.
- D. H. Olson, X. Yang and M. A. Camblor, *J. Phys. Chem. B*, 2004, **108**, 11044–11048.
- A. García-Sánchez, C. O. Ania, J. B. Parra, D. Dubbeldam, T. J. Vlugt, R. Krishna and S. Calero, *J. Phys. Chem. C*, 2009, **113**, 8814–8820.
- S. W. Rick, *J. Chem. Phys.*, 2004, **120**, 6085–6093.
- D. Dubbeldam, S. Calero, T. J. Vlugt, R. Krishna, T. L. Maesen and B. Smit, *J. Phys. Chem. B*, 2004, **108**, 12301–12313.
- A. Martín-Calvo, J. J. Gutiérrez-Sevillano, J. B. Parra, C. O. Ania and S. Calero, *Phys. Chem. Chem. Phys.*, 2015, **17**, 24048–24055.
- K. S. Deeg, J. J. Gutiérrez-Sevillano, R. Bueno-Pérez, J. B. Parra, C. O. Ania, M. Doblaré and S. Calero, *J. Phys. Chem. C*, 2013, **117**, 14374–14380.
- B. Zhakishcheva, J. J. Gutiérrez-Sevillano and S. Calero, *Sep. Purif. Technol.*, 2023, **306**, 122564.
- A. Martín-Calvo, J. J. Gutiérrez-Sevillano, I. Matito-Martos, T. J. H. Vlugt and S. Calero, *J. Phys. Chem. C*, 2018, **122**, 12485–12493.
- J. Pérez-Carbajo, J. B. Parra, C. O. Ania, P. J. Merklings and S. Calero, *ACS Appl. Mater. Interfaces*, 2019, **11**, 18833–18840.
- <https://webbook.nist.gov/chemistry>.
- D.-Y. Peng and D. B. Robinson, *Ind. Eng. Chem. Fundam.*, 1976, **15**, 59–64.
- Hydrogen and Syngas Production and Purification Technologies*, ed. K. Liu, C. Song and V. Subramani, Wiley, Hoboken, NJ, USA, 2010.
- C. Baerlocher, D. Brouwer, B. Marler and L. McCusker, *Database of Zeolite Structures*, <https://www.iza-structure.org/databases/>.
- K. C. Kemp, J. G. Min, H. J. Choi and S. B. Hong, in *New Developments in Adsorption/Separation of Small Molecules by Zeolites*, ed. S. Valencia and F. Rey, Springer Nature, Switzerland, 2020, vol. 184, pp. 1–30.
- S. Balestra, S. Hamad, A. Ruiz-Salvador, V. Domínguez-García, P. Merklings, D. Dubbeldam and S. Calero, *Chem. Mater.*, 2015, **27**, 5657–5667.
- P. Barrett, T. Boix, M. Puche, D. Olson, E. Jordan, H. Koller and M. Camblor, *Chem. Commun.*, 2003, 2114–2115.
- E. Pérez-Botella, M. Palomino, G. B. Báfero, H. O. Pastore, S. Valencia and F. Rey, *J. CO₂ Util.*, 2023, **72**, 102490.
- J. J. Gutiérrez-Sevillano, D. Dubbeldam, F. Rey, S. Valencia, M. Palomino, A. Martín-Calvo and S. Calero, *J. Phys. Chem. C*, 2010, **114**, 14907–14914.
- G. Cruciani, *J. Phys. Chem. Solids*, 2006, **67**, 1973–1994.
- G. Bera, P. Botella, J. Pellicer-Porres, D. Diaz-Anichtchenko, D. Errandonea, O. Gomis, R. Oliva, J. Ibañez, F. Alabarse, S. Valencia, F. Rey, A. Otero-de-la Roza and D. Santamaria-Perez, *Microporous Mesoporous Mater.*, 2024, **380**, 113317.
- J. van Heijst, A. Martín-Calvo and S. Calero, *Sep. Purif. Technol.*, 2024, **350**, 127895.

